JVI Journals.ASM.org

Impairment of HIV-1 cDNA Synthesis by DBR1 Knockdown

Alvaro E. Galvis,[a,b,c,d,e] Hugh E. Fisher,[b,c,d,e] Takayuki Nitta,[a,c,d] Hung Fan,[a,c,d] David Camerini[a,b,c,d,e]

Department of Molecular Biology & Biochemistry,[a] Division of Infectious Disease,[b] Cancer Research Institute,[c] Center for Virus Research,[d] and Institute for Immunology,[e] University of California, Irvine, California, USA

ABSTRACT

Previous studies showed that short hairpin RNA (shRNA) knockdown of the RNA lariat debranching enzyme (DBR1) led to a decrease in the production of HIV-1 cDNA. To further characterize this effect, DBR1 shRNA was introduced into GHOST-R5X4 cells, followed by infection at a multiplicity near unity with HIV-1 or an HIV-1-derived vector. DNA and RNA were isolated from whole cells and from cytoplasmic and nuclear fractions at different times postinfection. Inhibition of DBR1 had little or no effect on the formation of minus-strand strong-stop cDNA but caused a significant reduction in the formation of intermediate and full-length cDNA. Moreover, minus-strand strong-stop DNA rapidly accumulated in the cytoplasm in the first 2 h of infection but shifted to the nuclear fraction by 6 h postinfection. Regardless of DBR1 inhibition, greater than 95% of intermediate-length and full-length HIV-1 cDNA was found in the nuclear fraction at all time points. Thus, under these experimental conditions, HIV-1 cDNA synthesis was initiated in the cytoplasm and completed in the nucleus or perinuclear region of the infected cell. When nuclear import of the HIV-1 reverse transcription complex was blocked by expressing a truncated form of the mRNA cleavage and polyadenylation factor CPSF6, the completion of HIV-1 vector cDNA synthesis was detected in the cytoplasm, where it was not inhibited by DBR1 knockdown. Refinement of the cell fractionation procedure indicated that the completion of reverse transcription occurred both within nuclei and in the perinuclear region. Taken together the results indicate that in infections at a multiplicity near 1, HIV-1 reverse transcription is completed in the nucleus or perinuclear region of the infected cell, where it is dependent on DBR1. When nuclear transport is inhibited, reverse transcription is completed in the cytoplasm in a DBR1-independent manner. Thus, there are at least two mechanisms of HIV-1 reverse transcription that require different factors and occur in different intracellular locations.

IMPORTANCE

This study shows that HIV-1 reverse transcription starts in the cytoplasm but is completed in or on the surface of the nucleus. Moreover, we show that nuclear reverse transcription is dependent on the activity of the human RNA lariat debranchng enzyme (DBR1), while cytoplasmic reverse transcription is not. These findings may provide new avenues for inhibiting HIV-1 replication and therefore may lead to new medicines for treating HIV-1-infected individuals.

Human immunodeficiency virus type 1 (HIV-1) is the causative agent of AIDS. Like all retroviruses, HIV-1 must convert its RNA genome into DNA and then integrate its linear, double-stranded DNA into the cellular genome to program transcription of new viral RNA. The HIV-1 RNA- or DNA-dependent DNA polymerase reverse transcriptase (RT) synthesizes double-stranded viral DNA using the single-stranded RNA genome as the template (1). Reverse transcription is initiated from a tRNA primer bound at the primer binding site located 183 nucleotides from the 5′ end of the HIV-1 RNA genome (nucleotides 183 to 201 [1, 2]). Since the RNA genome is positive sense, the first product of reverse transcription is minus-sense cDNA. Initially, the cellular $tRNA^{Lys3}$ primes minus-strand strong-stop DNA synthesis, whereby the 5′ end of the viral positive-sense RNA genome is copied into minus-strand cDNA while the RNA template is degraded by the RNase H activity of RT (1, 2). After minus-strand strong-stop DNA synthesis, transfer of this nascent cDNA strand from the 5′ end of the genome to the 3′ end is required to continue synthesis of complete minus-strand cDNA (3–5) The precise mechanism of this strand transfer, however, has not been elucidated.

Retrotransposons are mobile genetic elements that resemble retroviruses and contain long terminal repeats (LTRs). They replicate and transpose via RNA intermediates. The Ty1 retroelement is among the best characterized of the retrotransposons of the yeast *Saccharomyces cerevisiae* (6). Using a genetic screen aimed at identifying cellular factors involved in Ty1 transposition, Chapman and Boeke found that debranching enzyme 1 (DBR1) plays a role in Ty1 transposition (7). DBR1 is a nuclear 2′-5′ phosphodiesterase that cleaves branch-point bonds in excised intron RNA lariats after mRNA splicing, facilitating turnover and recycling of lariat ribonucleotides. Yeast DBR1 mutant strains produce mature mRNAs but accumulate intron lariats, and they are defective in both Ty1 cDNA formation and transposition (6, 8, 9). Cheng and Menees (8) provided evidence that during cDNA synthesis the Ty1 RNA genome contains a 2′-5′ branch characteristic of an RNA lariat, although these data remain controversial (10). The location of this branch connecting the 5′ end of the genome to the 3′ nucleotide of the U3 region suggested that it may play a role during Ty1 cDNA synthesis by facilitating the transfer of nascent minus-strand cDNA from the 5′ end of the Ty1 RNA template to

Received 14 March 2014 **Accepted** 18 March 2014
Published ahead of print 26 March 2014
Editor: K. L. Beemon
Address correspondence to David Camerini, david.camerini@uci.edu.

doi:10.1128/JVI.00704-14

the 3′ R region (11). However, this possibility was subsequently challenged (10). The similarity of Ty1 to vertebrate retroviruses further raised the possibility that formation of an RNA lariat intermediate might be important for cDNA synthesis in the complex human retrovirus HIV-1.

The current model of minus-strand transfer is that RT initially copies the U5 and adjacent R region of the genome to form minus-strand strong-stop DNA, and at the same time, the RNase H function of RT degrades the 5′ end of the RNA in the resulting DNA-RNA hybrid (5). The free minus-strand strong-stop DNA is then able to hybridize with the 3′ end of the RNA genome via homology between its R region and the positive-sense R region in the 3′ end of the RNA genome (6). Marr and Telesnitsky, however, showed that as few as 5 bp of homology between the 5′ ends of the 5′ and 3′ R regions of Moloney murine leukemia virus (MMLV) is sufficient to allow minus-strand transfer (12). In contrast, much longer regions of homology were required for minus-strand transfer during first-strand cDNA synthesis at sites other than the U3-R boundary. This result suggested that something besides homology facilitates strand transfer after synthesis of complete minus-strand strong-stop DNA (12, 13). Moreover, in both MMLV and HIV-1, synthesis of complete minus-strand strong-stop DNA is strongly favored over early strand transfer (12, 13).

We have previously reported that short hairpin RNA (shRNA)-mediated knockdown of human DBR1 in HIV-1-infected cells inhibits the detection of late reverse transcription products and HIV capsid protein p24 at 24 h postinfection but has little effect on minus-strand strong-stop DNA synthesis. Moreover, this effect can be reversed if cells are cotransfected with a DBR1 expression plasmid (14). These results are consistent with a mechanism in which the 5′ and 3′ ends of the genomic RNA are brought together during reverse transcription into an RNA lariat-like structure in the absence of sequence homology; if a lariat-like intermediate is formed, resolution of the structure by DBR1 would be important for the completion of cDNA synthesis, since lariat branch points cause RT pausing or termination (15). Alternatively, DBR1 might play a different role in HIV-1 reverse transcription independent of lariat resolution.

In the present study, we confirmed our previous results that DBR1 inhibition decreases the amount of detectable intermediate and late products of reverse transcription in cells infected by an HIV-1-based vector or a clinical HIV-1 isolate but that it has minimal effect on the formation of minus-strand strong-stop DNA. We extended these studies by performing cell fraction experiments and detected the great majority of intermediate and late reverse transcription products in the nuclear or perinuclear region, indicating that under the conditions employed at a multiplicity of infection (MOI) of nearly 1, reverse transcription is initiated in the cytoplasm but completed in the nuclear fraction. When HIV-1 nuclear entry was blocked in cells expressing a truncated form of cleavage and polyadenylation factor 6 (CPSF6) known as CPSF6-358, intermediate and full-length cDNA synthesis was detected in the cytoplasm; cytoplasmic cDNA synthesis was not dependent on DBR1. Refinements of the cell fractionation procedure indicated that the completion of cDNA synthesis can occur either in the nucleus or in the perinuclear region. Taken together, the results indicate that strand transfer and the completion of HIV-1 cDNA synthesis predominantly take place in the nucleus or perinuclear region but that it can also take place in the cytoplasm. Nuclear completion of cDNA synthesis is dependent on DBR1, while the completion of cDNA synthesis in the cytoplasm is not. These results provide evidence of two alternate mechanisms of HIV-1 reverse transcription.

MATERIALS AND METHODS

Construction of small interfering RNA expression vectors. The shRNA expression vector pHyper was a gift of Vicente Planelles (14). The vector expresses a 23-nucleotide hairpin-type shRNA with a 6-nucleotide loop that has been extensively described (17, 18). The 19-nucleotide DBR1 sequence D4 (CTTGCTGTGCTGCGGCGAC) was used to create the DBR1 shRNA plasmid designated pHyper-D4 (D4). The 19-nucleotide DBR1 triple-mismatch sequence M4 (CTTCCTGTACTGCAGCGAC) was used to create the DBR1 shRNA plasmid designated pHyper-M4 (M4).

Preparation and titration of HIV vector stocks. The pCMVΔR8.2 and pMDG plasmids encode HIV-1 structural proteins and the vesicular stomatitis virus G protein (VSV-G), respectively, and have been extensively described (19, 20). The pHR-E plasmid contains a truncated HIV-1 *env* gene and the HIV-1-derived *cis*-acting sequences necessary for packaging reverse transcription and integration. Viral vector stocks were prepared by triple transfecting human embryonic kidney 293T cells (3.0×10^7 cells in 500-cm^2 plates) with 75 μg of plasmids pHR-E, pCMVΔR8.2, and pMDG coprecipitated with calcium phosphate. At 2 days posttransfection, the culture supernatant was collected, filtered, and frozen at −80°C until needed. VSV-G-pseudotyped HIV-1 vector virions in the supernatant were quantified by infecting cells for 24 h, followed by quantitative real-time PCR (qPCR) of vector DNA.

Preparation and titration of HIV-1 stocks. The HIV-1 biological clone ACH 337.40.1c1 was obtained from the Amsterdam cohort study (21). Viral stocks were amplified by infection of healthy donor peripheral blood mononuclear cells (PBMCs) that had been prestimulated for 2 days with phytohemagglutinin. One half of the virus-containing supernatants was removed every 2 days and replaced with fresh medium containing interleukin-2. Fresh stimulated PBMCs were added at 7 days postinfection if the viral titers of the collected supernatants had not peaked. Virus-containing supernatants were aliquoted, filtered, and frozen at −80°C until needed. The amount of virus in the supernatant was determined by infecting cells for 24 h, followed by qPCR of HIV-1 DNA. Virus stocks were supplemented with $MgCl_2$ to 10 mM and treated with 10 μg/ml DNase I at 37°C for 30 min prior to infection.

Cell culture, transfection, and infection. GHOST-R5X4 is a HOS-derived cell line that is stably transduced with the MV7neo-T4 retroviral vector, which is stably cotransfected with the HIV-2 LTR driving humanized green fluorescent protein, and that coexpresses both CCR5 and CXCR4 (22). GHOST-R5X4 cells were cultured in Iscove's modified Dulbecco's medium (IMDM) containing 10% fetal bovine serum (FBS), 50 μg/ml gentamicin, and 500 μg/ml G418. Human embryonic kidney 293T cells were cultured in IMDM supplemented with 10% FBS and 50 μg/ml gentamicin. HeLa.LPCX and HeLa.LPCX-HA-CPSF6-358 cells were gifts from Vineet N. KewalRamani and have been well characterized (23). HeLa cell lines were cultured in IMDM containing 10% FBS, 50 μg/ml gentamicin, and 1 μg/ml puromycin. GHOST-R5X4 and HeLa cell lines were seeded overnight at 10^6 cells per well in a six-well plate prior to transfection. Cells were transfected using Lipofectamine (Invitrogen), according to the manufacturer's instructions, at a ratio of 1 μl of Lipofectamine per microgram of plasmid DNA. At 48 h after transfection, cells were infected with DNase I-treated viral stocks of either VSV-G-pseudotyped pHR-E or a clinical HIV-1 clone. Cells were harvested for DNA or RNA isolation and fractionated into total, cytoplasmic, and nuclear fractions.

NP-40 fractionation. At appropriate times after the start of the infection, cells were harvested by washing twice with phosphate-buffered saline (PBS); next, the cells were trypsinized for 5 min at 37°C and collected by low-speed centrifugation. For total DNA and RNA isolation, the cells were resuspended in PBS. For separation of cytoplasmic and nuclear nucleic

acids, cells were resuspended in TMK (25 mM Tris-HCl, pH 7.4, 1 mM $MgCl_2$, 5 mM KCl) and plasma membranes were disrupted by incubating for 5 min on ice in TMK containing 0.5% Nonidet P-40 (NP-40). The nuclei were then pelleted at 228 × *g* and 4°C for 5 min, and the supernatant, considered the cytoplasmic fraction, was clarified by centrifugation at 5,000 × *g* for 5 min in 4°C before further processing. Nuclei were resuspended in S1 buffer (250 mM sucrose, 10 mM $MgCl_2$), layered over S2 buffer (350 mM sucrose, 0.5 mM $MgCl_2$), and centrifuged at 1,430 × *g* for 5 min at 4°C. The supernatant was removed, and the nuclei were once more resuspended in S1 buffer, layered over S2 buffer, and centrifuged at 1,430 × *g* for 5 min at 4°C. This process was repeated one more time before further processing. The nuclear pellet and cytoplasmic fraction were then used for nucleic acid extractions.

Double-detergent fractionation of cells. At appropriate times after the start of the infection, cells were harvested by washing twice with cold PBS, trypsinized for 15 min at 4°C, and collected by low-speed centrifugation. For total DNA and RNA isolation, the cells were resuspended in PBS. For separation of cytoplasmic and nuclear nucleic acids, cells were resuspended in the hypotonic buffer RSB (10 mM NaCl, 10 mM Tris-HCl, pH 7.4, 1.5 mM $MgCl_2$) and incubated for 10 min on ice, and plasma membranes were disrupted with 10 strokes of a glass Dounce homogenizer (B pestle). The nuclei were separated by centrifugation at 1,600 × *g* for 5 min, and the supernatant fraction was saved for use as the cytoplasmic fraction. The nuclei were resuspended in RSB and centrifuged at 1,600 × *g* for 5 min, and the supernatant fraction was combined with the previous fraction. The combined RSB supernatant fractions were designated the cytoplasmic fraction, and the nuclear pellet was designated the nuclear plus perinuclear (N+P) fraction. The two fractions were then processed for nucleic acid extractions. To remove perinuclear material from the nuclei, the N+P fraction pellets were again resuspended in RSB and a mixture of two detergents was added to the nuclear suspension to give final concentrations of 0.5% sodium deoxycholate and 1% Tween 40. The nuclear suspension was vortexed and centrifuged at 1,600 × *g* for 5 min, and the supernatant fraction was added to the previous cytoplasmic fraction to give the cytoplasmic plus perinuclear (C+P) fraction (24, 25). The nuclear pellet and C+P fractions were then processed for nucleic acid extractions.

Western blot analysis. Cytoplasmic and nuclear fractions isolated from HeLa cells were subjected to SDS-PAGE, transferred to a polyvinylidene difluoride membrane, and then incubated with TBS-T (0.05 M Tris, 0.138 M NaCl, 0.0027 M KCl, 0.05% Tween 20) containing 5% skim milk (Carnation; Nestle) at room temperature for 1 h. The membranes were probed with primary antibodies directed to lamin A/C (1:2,000; catalog no. 2032; Cell Signaling), beta-tubulin (1:2,000; catalog no. 2146; Cell Signaling), nucleoporin Nup214 (1:400; catalog no. A300-717A; Bethyl Laboratories), or nucleoporin Nup98 (1:1,000; catalog no. 2598; Cell Signaling) at 4°C for overnight. Subsequently, the membranes were washed with TBS-T four times and exposed to the secondary antibodies at room temperature for 2 h. Horseradish peroxidase-conjugated anti-rabbit IgG antibody (Thermo Scientific) was diluted in TBS-T and incubated with the membranes for 2 h at room temperature, prior to four additional 10-min washes. SuperSignal West Femto chemiluminescent substrate (Thermo Scientific) was used to detect the signals. Images were captured with a FluorChem SP digital imaging system (Alpha Innotech).

Nucleic acid extraction. For all DNA extractions, the samples were treated with ice-cold lysis buffer (10 mM Tris-HCl, pH 8.0, 1 mM EDTA, 0.1% SDS) and incubated with proteinase K at 55°C for 16 h. The DNA was sheared 15 times through a 21-gauge needle, followed by a DNase-free RNase treatment for 1 h at 37°C. The DNA was precipitated with isopropanol and washed with 70% ethanol. DNA pellets were resuspended in 10 mM Tris-HCl, pH 7.4, 1 mM EDTA (TE) and stored at 4°C (26). For all RNA extractions, the samples were resuspended in TRIzol reagent and processed according to the manufacturer's instructions. The samples were stored at −80°C until needed. The accuracy of the nucleocytoplasmic separation was verified by qPCR using nuclear, mitochondrial, and 45S ribosomal subunit primers.

Quantitative PCR. DNA samples were diluted 1 to 10 in distilled H_2O (dH_2O) and incubated at 98°C for 20 min, followed by immediate cooling on ice. Each PCR mixture contained 7.5 μl SYBR green PCR master mix (Fermentas), 2 μl of template, and 1 μM each primer in a 15-μl reaction volume. HIV-1-specific primers AA55 (CTGCTAGAGATTTTCCACAC TGAC; nucleotides 635 to 612) and M667 (GGCTAACTAGGGAACCCA CTG; nucleotides 496 to 516) were used to detect minus-strand strong-stop DNA. Primers env1 (GGCAGGGATACTCACCCTTATCG; nucleotides 8337 to 8360) and env2 (GGATTTCCCACCCCCTGCGT CCC; nucleotides 8590 to 8566) were used to detect intermediate-length reverse transcription products. Primers M661 (CCTGCGTCGAGAGAG AGCTCCTCTGG; nucleotides 695 to 672) and M667 were used to detect the complete synthesis of HIV-1 cDNA. The number of copies of HIV-1 DNA in the total and nuclear fractions was normalized against the number of copies of β-globin DNA using primers LA1 (ACACAACTGTGTT CACTAGC) and LA2 (CAACTTCATCCACGTTCACC) directed to the human β-globin gene to obtain the number of HIV-1 DNA copies per cell (12, 14). For cytoplasmic fractions, the number of HIV-1 copies was normalized against the number of copies of mitochondrial DNA using primers MitouaF (GATCACAGGTCTATCACCCT; nucleotides 1 to 20) and MitouaR (GGATGAGGCAGGAATCAAAG; nucleotides 132 to 151) to obtain the number of HIV-1 DNA copies per mitochondrial genome. qPCR was performed in triplicate for each sample using an ABI Prism 7900HT sequence detection system (PE Applied Biosystems) for amplification and detection. PCR conditions were as follows: initial denaturation at 95°C for 10 min and then 40 rounds of cycling at 95°C for 15 s and 60°C for 60 s. The purity of the NP-40 nucleocytoplasmic fraction was verified by comparing the number of mitochondrial DNA copies detected in the nuclear fraction and the number of β-globin DNA copies detected in the cytoplasmic fraction with the respective number of copies found in the total cell lysate. The purity of the double-detergent nucleocytoplasmic fraction was verified by comparing the number of 45S rRNA copies detected in the cytoplasmic fraction and the number of mitochondrial DNA copies detected in the nuclear fraction with the number of copies found in the total cell lysate. The 45S rRNA primers utilized were 45SrRNAF (GAACGGTG GTGTGTCGTT; nucleotides 851 to 868) and 45SrRNAR (GCGTCTC GTCTCGTCTCACT; nucleotides 961 to 980) (27).

Quantitative RT-PCR. RNA was quantified by measuring the absorbance at 260 nm. RNA (2.5 μg) was treated with 2 units of DNase I (Fermentas) in a volume of 10 μl to remove contaminating DNA, followed by heat inactivation of the enzyme (37°C for 20 min, 60°C for 5 min). RNA was reverse transcribed using a first-strand cDNA synthesis kit (Fermentas) following the manufacturer's instructions. The total cDNA volume of 20 μl was frozen until real-time quantitative PCR was performed. After thawing for PCR experiments, the cDNA was diluted 1 to 10 in dH_2O, and 2 μl of diluted cDNA was used for each PCR. Real-time quantitative PCR was performed as described in the previous section. Each PCR mixture, prepared in triplicate, contained 7.5 μl SYBR green PCR master mix (Fermentas) and 1 mM each primer for glyceraldehyde-3-phosphate dehydrogenase (GAPDH), human DBR1, the HIV-1 5′ RNA genome region (primers M661 and M667), and the HIV-1 3′ RNA genome region (primers env1 and env2). The forward and reverse primer sequences for amplifying DBR1 were GGAAACCATGAAGCCTCAAA (nucleotides 247 to 266) and CCGATCCTTACACCTCGGTA (nucleotides 444 to 425), respectively. The forward and reverse primer sequences for amplifying GAPDH were CAAATTCCATGGCACCGTCAA (nucleotides 264 to 284) and GTTGCTGTAGCCAAATTCGTTGT (nucleotides 314 to 333), respectively. The relative HIV-1 copy number was calculated by dividing the HIV-1 copy number (determined from the appropriate standard curve) by the GAPDH copy number.

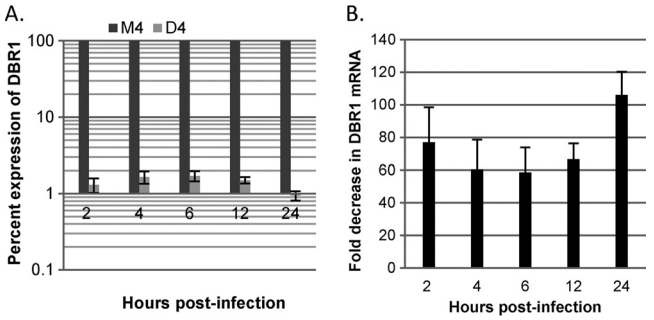

FIG 1 Inhibition of DBR1. GHOST-R5X4 cells were transfected with 8.4 μg of either D4 or M4 DNA per well of a six-well plate using Lipofectamine (Invitrogen). Forty-eight hours later, the cells were infected with a DNase-treated HIV-1 vector (HR-E). Two to 24 h later, the cells were lysed and RNA was isolated for quantitative reverse transcription-PCR to evaluate the inhibition of DBR1. For the reverse transcription reaction, a total of 2.5 μg of RNA was used per sample. The data represent those from three independent quantitative reverse transcription-PCR time course experiments processed in triplicate. Error bars denote standard deviations from the means. (A) Percent expression of DBR1 in D4-treated cells, in contrast to maximal expression (100%) in M4-treated cells; (B) average fold DBR1 knockdown compared to that for the mismatch control, M4.

RESULTS

DBR1 shRNA suppression of DBR1 mRNA. To study the role of DBR1 in HIV reverse transcription, an improved shRNA knockdown construct was generated. A DBR1 shRNA and a corresponding control containing 3 nucleotides mismatched in the targeting sequence (triple-mismatch control) were designed and inserted into pHyper, which expressed the shRNAs under the control of the H1 RNA promoter. pHyper carrying DBR1 shRNA was designated D4, and pHyper carrying triple-mismatch shRNA was designated M4. GHOST-R5X4 cells were transfected with the two plasmids via Lipofectamine, and 48 h later, DBR1 mRNA levels were analyzed by quantitative reverse transcription-PCR. DBR1 expression was knocked down to an average of 1.24% in D4-treated cells compared to that in cells treated with the control, M4 (Fig. 1A). Moreover, DBR1 mRNA levels were decreased an average of 74-fold (range, 59- to 106-fold) at between 50 and 72 h posttransfection of pHyper-D4, but they were not affected by transfection of M4 (Fig. 1B).

DBR1 shRNA suppresses HIV-1 reverse transcription but not strong-stop cDNA synthesis. To more precisely determine the stage at which HIV-1 replication is inhibited by degradation of DBR1 mRNA, we transfected GHOST-R5X4 cells with DBR1 shRNA D4 or the triple-mismatch control M4 for 48 h and then infected the cells with the VSV-G-pseudotyped HIV-1 vector pHR-E at an MOI of 1 and harvested the cells at 2 to 24 h postinfection. Cells were lysed, and DNA was isolated and analyzed by qPCR for HIV-1 cDNA products (Fig. 2). The oligonucleotide primers M667 and AA55, specific for the R and U5 regions of the HIV-1 LTR, respectively, were used to detect early reverse transcription products, also known as strong-stop DNA. The *env* primers env1 and env2 were designed to detect intermediate-length reverse transcription products formed soon after minus-strand cDNA transfer to the 3′ end of the template, while the LTR R region and *gag* primers M667 and M661 were chosen to detect completely synthesized viral cDNA (Fig. 2A). The number of copies of HIV-1 cDNA was normalized against the number of copies of β-globin DNA to obtain the absolute number of HIV-1 cDNA copies per cell.

Strong-stop cDNA synthesis was not affected by DBR1 shRNA until 4 h postinfection and was inhibited only modestly (by one-third) at later times (Fig. 2B; see below). In contrast, the levels of intermediate and late products of reverse transcription were substantially decreased in the presence of DBR1 shRNA at all time points postinfection at which they were detectable ($P < 0.001$; Fig. 2C and D). Furthermore, as time progressed, the difference between the numbers of intermediate and full-length HIV-1 vector cDNA copies in D4- versus M4-treated cells increased to a maximal difference of 8.5-fold ($P = 3.1 \times 10^{-6}$) and 7.6-fold ($P = 5.9 \times 10^{-10}$), respectively, at 24 h postinfection. These results indicate that DBR1 knockdown inhibits cDNA synthesis at a step during or after minus-strand transfer, consistent with the findings of our previous studies (14).

As noted above, HIV-1 strong-stop DNA synthesis was not affected by DBR1 knockdown until 4 h postinfection, but there was statistically significant inhibition starting at 4 h postinfection, and this increased to a 1.5-fold effect at 24 h (Fig. 2B). This inhibition likely reflected the fact that a second LTR is generated as a late step in reverse transcription, and the strong-stop primers would detect the sequences in both LTRs. Since DBR1 knockdown inhibited the intermediate and late products of reverse transcription, the second LTR also would not be generated, leading to the observed effect on strong-stop DNA synthesis after 4 h. Thus, these results indicate that DBR1 is not required for initial strong-stop cDNA synthesis. Instead, DBR1 shRNA inhibits the synthesis of intermediate and late products of reverse transcription, perhaps by decreasing the efficiency of minus-strand transfer or of cDNA synthesis after strand transfer. In contrast, DBR1 knockdown in the vector-producing cells had no effect on reverse transcription in target cells, indicating that DBR1 does not mediate its effects by being packaged into virions (not shown).

Reverse transcription is initiated in the cytoplasm and completed in the nucleus. We next investigated the cellular location of reverse transcription. The conventional view is that retroviral reverse transcription is completed in the cytoplasm, followed by transport of the completed viral DNA as a preintegration complex into the nucleus. However, there have been relatively few studies addressing this question with quantitative techniques such as qPCR. We therefore infected GHOST-R5X4 cells previously transfected with the D4 knockdown shRNA or the M4 mismatch control with the HIV vector HR-E at an MOI of 1. At different times after infection, the cells were harvested and lysed with 1% NP-40, followed by separation into nuclear and cytoplasmic fractions. qPCR for the different reverse transcription products was then conducted. The efficiency of the NP-40 fractionation procedure was assessed by qPCR for genomic β-globin DNA (nuclear) and human mitochondrial DNA (cytoplasmic). After fractionation, 95 to 99% of the mitochondrial DNA was in the cytoplasmic fraction and 98 to 99% of the β-globin DNA was in the nuclear fraction (data not shown). In these experiments, infection at a low MOI was employed to approximate the likely situation *in vivo* and to avoid the potential saturation of cell transport mechanisms that could occur during infection at a high MOI.

Analysis of HIV-1 vector cDNA in subcellular fractions demonstrated that at 1 and 2 h postinfection, strong-stop cDNA was predominantly found in the cytoplasm in control (M4-transfected) cells (Fig. 3A). By 4 h postinfection, however, almost 50%

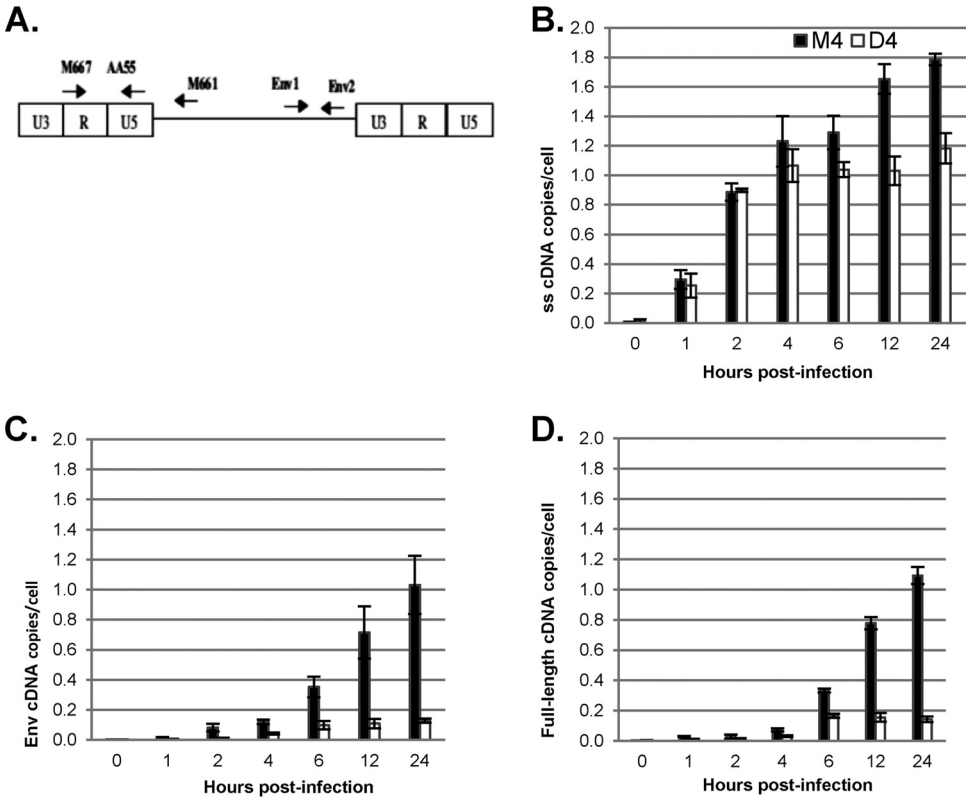

FIG 2 DBR1 shRNA inhibits the completion of HIV-1 reverse transcription. GHOST-R5X4 cells were transfected with D4 or M4 for 48 h, followed by infection with a DNase-treated HIV-1 vector (HR-E). Zero to 24 h later, the cells were lysed and DNA was isolated for qPCR to evaluate the synthesis of HIV-1 cDNA. The number of copies of HIV-1 was normalized to the number of copies of β-globin. The data represent those from three independent time course experiments processed in triplicate. Error bars denote the standard deviations from the means. Differences between D4- and M4-treated cells were significant by Student's *t* test ($P < 0.01$) at 6, 12, and 24 h postinfection for strong-stop DNA and at all nonzero time points for intermediate and full-length cDNA. (A) Locations of primers; (B) the oligonucleotide primers M667/AA55 specific for the R/U5 region of the LTR were used to detect early reverse transcripts (strong-stop [ss] DNA); (C) *env* primers env1/env2 were used to detect intermediate reverse transcripts; (D) LTR/*gag* primers M667/M661 were chosen to detect complete, full-length viral cDNA.

of the strong-stop cDNA was associated with the nuclear fraction, and at later times, nuclear strong-stop cDNA accumulated while the level of cytoplasmic strong-stop cDNA decreased. This was consistent with the initiation of cDNA synthesis in the cytoplasm. Surprisingly, intermediate and full-length products of reverse transcription were found almost exclusively in the nuclear fraction at all times (Fig. 3C and E). This suggested that under these conditions, reverse transcription was completed after the reverse transcription complex (RTC) was transported to the nucleus. Similar results were obtained when a clinical isolate of HIV-1 was used to infect GHOST-R5X4 cells (Fig. 4) and when the VSV-G-pseudotyped HR-E vector was used to infect HeLa cell-derived cell lines at a low MOI, as shown below (see Fig. 7 to 10). These data strongly suggest that regardless of viral entry pathways, transport of the RTC to the nucleus is coincident with steps in reverse transcription that occur after strong-stop cDNA synthesis.

Results of infection of GHOST-R5X4 cells in which DBR1 was knocked down are also shown in Fig. 3B, D, and F. As described above, the initial cytoplasmic accumulation of strong-stop DNA was largely unaffected by DBR1 shRNA expression. In contrast, DBR1 shRNA treatment strongly inhibited the formation of products after the minus-strand template switch; this effect was observed in the nuclear fractions. Consistent with the results shown in Fig. 2 and our previous work (14), nuclear *env* region cDNA synthesis was inhibited 8.1-fold and nuclear full-length cDNA synthesis was inhibited 8.2-fold by DBR1 shRNA at 24 h postinfection. Moreover, these results are also consistent with the hypothesis that DBR1, which is a nuclear factor, may facilitate HIV-1 cDNA synthesis during or after minus-strand transfer.

Subcellular localization and degradation of the HIV-1 vector RNA genome. We also followed the effects of DBR1 knockdown on degradation of the HIV-1 vector RNA genome in the cytoplasmic and nuclear fractions of infected cells. GHOST-R5X4 cells were transfected with D4 or the control M4 for 48 h and then infected with the VSV-G-pseudotyped HR-E and harvested at 2, 6, and 12 h postinfection. The cells were lysed and fractionated, RNA was isolated, and vector RNA was quantified by quantitative reverse transcription-PCR (Fig. 5). We utilized the oligonucleotide primers env1 and env2 to detect the 3′ region of the HIV-1 vector genomic RNA, while primers M667 and M661 were chosen to detect the 5′ region of the vector genomic RNA (including the strong-stop templates R and U5) (Fig. 2A). The 5′ region of the vector genome was rapidly degraded, consistent with early reverse transcription of minus-strand strong-stop cDNA and degradation of the template RNA by the RNase H activity of reverse transcriptase (Fig. 5A). As expected, DBR1 shRNA had no effect at any time on the degradation of the 5′ region of the vector genome, since knockdown of DBR1 did not inhibit minus-strand strong-stop

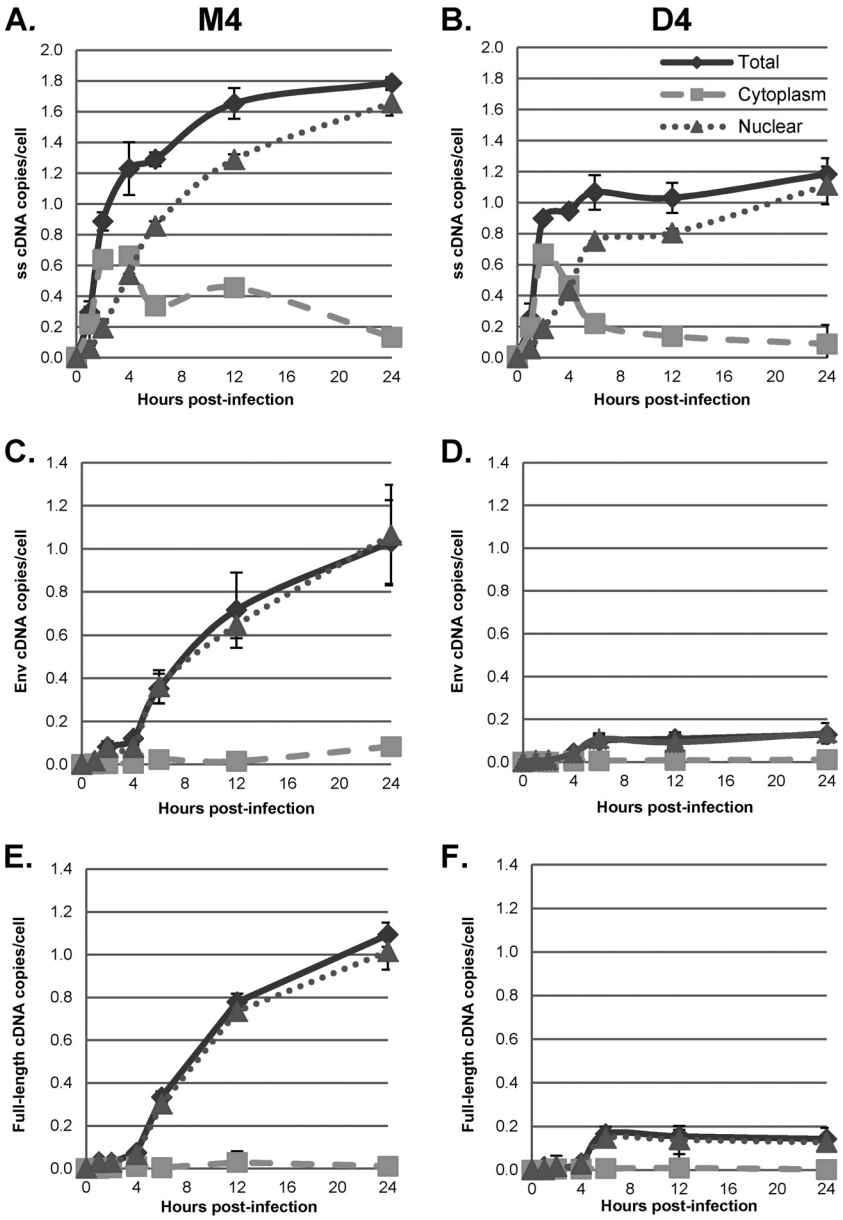

FIG 3 Subcellular localization of reverse transcription products. GHOST-R5X4 cells were transfected with D4 or M4 for 48 h, followed by infection with a DNase-treated HIV-1 vector (HR-E). Zero to 24 h later, the cells were either fractionated with a hypotonic buffer or lysed to prepare whole-cell fractions. DNA was isolated to evaluate the synthesis of HIV-1 cDNA using the primers for strong-stop DNA (A and B), *env* DNA (C and D), and full-length DNA (E and F) shown in Fig. 2A. (A, C, and E) Infection of M4-transfected cells; (B, D, and F) infection of D4-transfected cells. The viral DNA copy numbers were normalized to the numbers of copies of either the β-globin DNA (for the total and nuclear fractions) or mitochondrial DNA (for the cytoplasmic fraction) standards. Error bars denote the standard deviations from the means. The data represent those from three independent time course experiments processed in triplicate.

DNA synthesis (Fig. 5B). When the 3′ region of the vector RNA was analyzed in control (M4) cells, most of it was cytoplasmic at 2 h, but at later times it was essentially all nuclear. Compared to the rate of degradation of 5′ RNA, the rate of degradation of 3′ RNA was lower, with greater than 80% of total 3′ RNA still being present at 6 h postinfection, at which time it was nearly all nuclear (Fig. 5C, open bars). These results were consistent with reverse transcription of the 3′ end of the vector RNA (after strand transfer) in the nucleus at between 6 and 12 h, accompanied by degradation of the template RNA. In contrast, knockdown of DBR1 prevented degradation of the 3′ region of the HIV-1 vector, consistent with its inhibition of late reverse transcription (Fig. 5D). Furthermore, under DBR1-knockdown conditions, the 3′ region of the vector genome was found almost exclusively in the nuclear fraction at 6 h or later. This is again consistent with the transport of RTCs that have initiated reverse transcription in the cytoplasm to the nucleus, where the completion of reverse transcription takes place; if DBR1 is not available, the completion of reverse transcription and degradation of template RNA in the nucleus do not occur.

Blocking transport of HIV-1 to the nucleus results in the completion of reverse transcription in the cytoplasm. To further investigate the relationship of the nuclear transport of the RTC

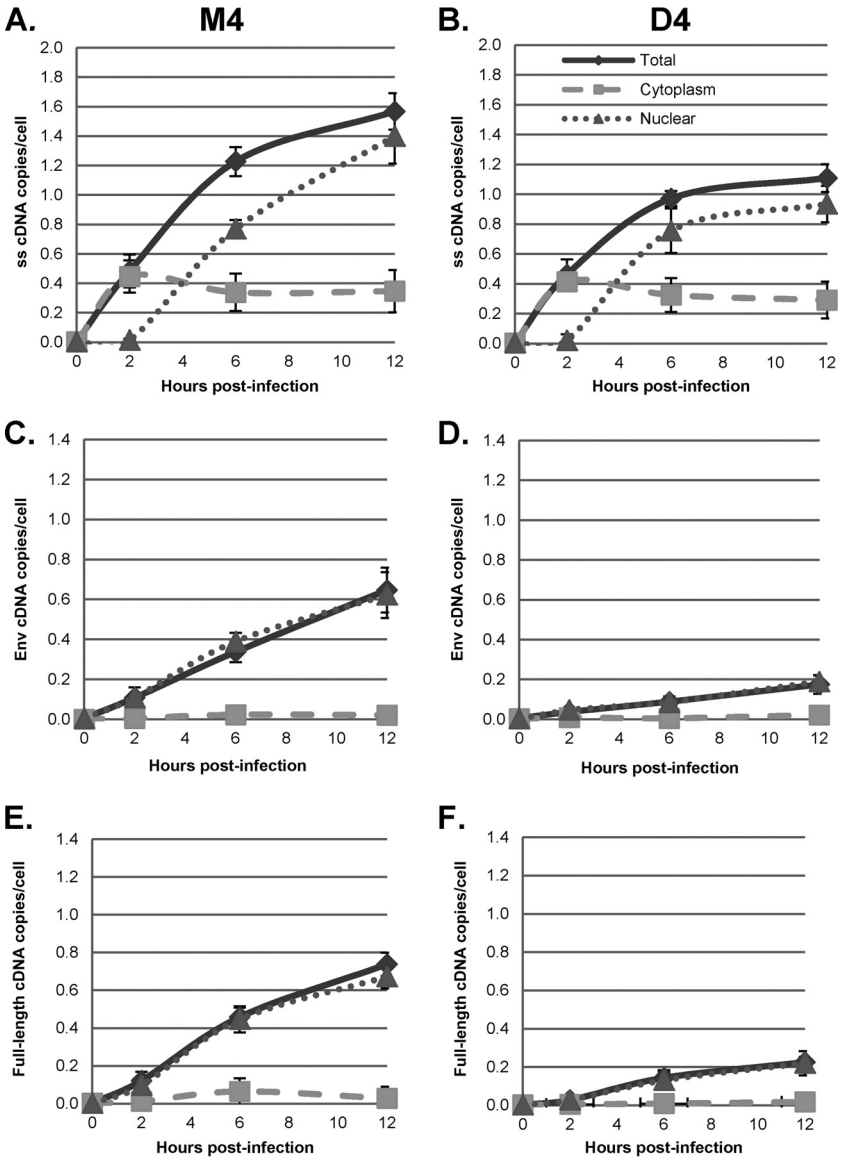

FIG 4 Reverse transcription of a clinical HIV-1 isolate is inhibited by DBR1 depletion and completed in the nucleus. GHOST-R5X4 cells were transfected with D4 or M4 for 48 h and then infected with the HIV-1 clinical clonal isolate ACH 337.40.1c1 and harvested at 2 to 12 h postinfection. The cells were lysed and fractionated, and DNA was isolated to evaluate the synthesis of HIV-1 cDNA by qPCR. The analysis was the same as that described in the legend to Fig. 3. Error bars denote the standard deviations from the means. The data represent those from three independent time course experiments processed in triplicate.

and the completion of reverse transcription, we employed a HeLa-derived cell line that expresses a truncated dominant negative form of the cleavage and polyadenylation factor 6 (CPSF6) known as CPSF6-358 (23). Lee et al. have shown that expression of CPSF6-358 blocks HIV-1 infection at the level of nuclear transport (23). We transfected HeLa cells expressing CPSF6-358 with D4 or the M4 control for 48 h and then infected the cells with VSV-G-pseudotyped HIV-1 vector HR-E and harvested the cells at 2 to 24 h postinfection. Cells were fractionated into total, cytoplasmic, and nuclear fractions, and synthesis of HIV-1 cDNA was measured by qPCR, as described above. As previously reported (23), the expression of CPSF6-358 caused the accumulation of strong-stop cDNA in the cytoplasm, which did not occur in infected control HeLa cells (Fig. 6A and B). At later times, there was low-level transfer of strong-stop cDNA to the nucleus, which may have resulted from the fact that these cells were dividing. In CPSF6-358 cells transfected with the D4 plasmid for DBR1 knockdown, there was little effect on the initial amount of total strong-stop cDNA, which was largely retained in the cytoplasm (Fig. 6C). As described above, the total amounts of strong-stop cDNA at later times were reduced due to the lack of generation of the second LTR during late reverse transcription in the nucleus.

In contrast, when intermediate and late reverse transcription products (*env* and *gag*) were studied, blockage of nuclear import by CPSF6-358 had two effects. First, the overall amounts of reverse transcripts were modestly reduced (25 to 35%; Fig. 7A versus C and B versus D). Second, and more strikingly, in CPSF6-358 cells, intermediate and late cDNA products accumulated in the cytoplasm (Fig. 7C and D). Thus, when the nuclear transport of RTCs is blocked, the completion of reverse transcription can occur in

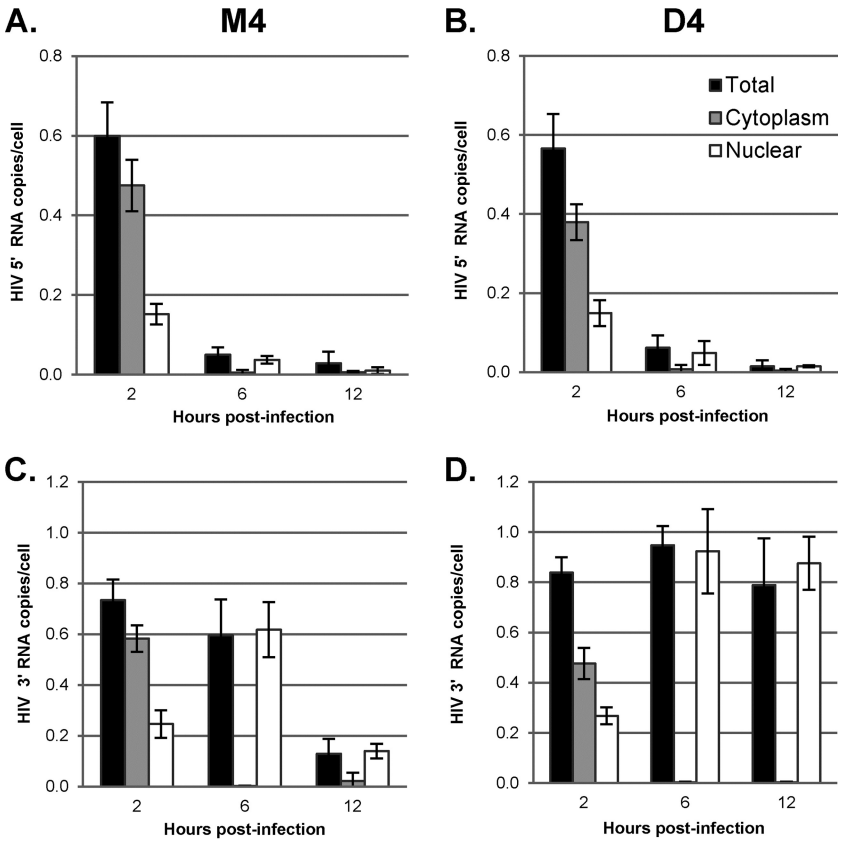

FIG 5 Degradation and subcellular localization of the viral RNA genome during reverse transcription. GHOST-R5X4 cells were transfected with D4 or M4 for 48 h, followed by infection with a DNase-treated HIV-1 vector (HR-E). Two to 12 h later, the cells were either fractionated utilizing the NP-40 protocol or lysed to prepare whole-cell fractions. RNA was isolated for RT-qPCR to evaluate the degradation and subcellular localization of the viral RNA genome during reverse transcription. The data were normalized to the GAPDH copy number. Error bars denote the standard deviations from the means. The data represent those from three independent time course experiments processed in triplicate. LTR/*gag* primers M667/M661 were chosen to detect the 5′ region of the viral RNA genome in M4-treated cells (A) and D4-treated cells (B). The *env* primers env1/env2 were used to detect the 3′ region of the viral RNA genome in M4-treated cells (C) and D4-treated cells (D).

the cytoplasm, although the overall efficiency of reverse transcription is reduced somewhat. The effects of DBR1 knockdown on reverse transcription in CPSF6-358-expressing cells are also shown in Fig. 7E and F. Knockdown of DBR1 further reduced the total levels of intermediate and late reverse transcription products, with maximal effects of 1.7- and 2.1-fold, respectively, at 24 h postinfection ($P = 0.016$ and $P = 6.42 \times 10^{-6}$, respectively). Interestingly DBR1 knockdown did not affect the accumulation of intermediate and late products in the cytoplasm ($P = 0.25$ and $P = 0.12$, respectively, at 24 postinfection). In contrast, DBR1 knockdown caused a significant reduction of nuclear post-strong-stop reverse transcription products: 2.8-fold ($P = 0.0022$) and 4-fold ($P = 0.0025$), respectively, for intermediate and late products at 24 h postinfection. Taken together, the data point to two different mechanisms of reverse transcription that are subcellular compartment specific. Under normal circumstances under the conditions used here, reverse transcription is initiated in the cytoplasm, but it is completed in the nucleus, where DBR1 is required. On the other hand, reverse transcription can also be completed in the cytoplasm when nuclear transport is inhibited; cytoplasmic completion of reverse transcription does not require DBR1.

Double-detergent fractionation identifies full-length cDNA products in both the cytoplasm and nucleus. The cell fractionation procedure used in the preceding experiments used lysis of cells by a nonionic detergent (0.5% NP-40). However, this procedure likely did not completely remove perinuclear material from the nuclear fraction. To address this concern, we employed a different procedure for cell fractionation. It has previously been shown that the treatment of nuclei with a mixed anionic-ionic double detergent (Tween 80-deoxycholate) can remove perinuclear material and the outer nuclear membrane from nuclei (24, 25). In this procedure, cells were lysed by hypotonic swelling and Dounce homogenization, the nuclear pellets were washed with double detergent, and the resulting supernatant was combined with the cytoplasmic supernatants; this resulted in two fractions: nuclei free of perinuclear material and a combined cytoplasmic-perinuclear (C+P) fraction. The success of the double-detergent fractionation procedure (as described in Materials and Methods) was assayed by measuring the levels of the 45S ribosomal precursor RNA in the nuclear fraction via RT-qPCR and of the mitochondrial DNA in the cytoplasmic fraction via qPCR as well as by Western blotting for nuclear and cytoplasmic proteins. Beta-tubulin was used as a cytoplasmic marker, and lamin A/C was used as a nuclear marker. In addition, the nucleoporin Nup98 is located on the nuclear side of the nuclear pore (29), while Nup214 is located on the cytoplasmic (perinuclear) side of the nuclear pore

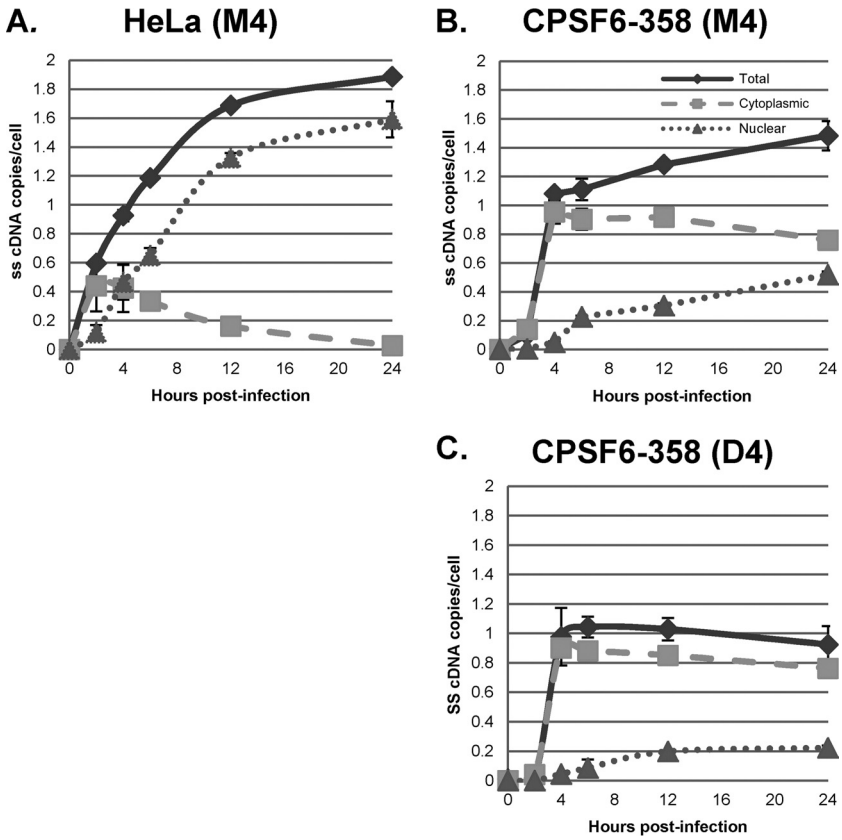

FIG 6 Effects of nuclear entry and DBR1 inhibition on HIV-1 strong-stop cDNA synthesis. HeLa.LPCX cells were transfected with M4, and HeLa.LPCX-HA-CPSF6-358 cells were transfected with D4 or M4 for 48 h, followed by infection with a DNase-treated HIV-1 vector (HR-E). Zero to 24 h later, the cells were either fractionated into nuclear and cytoplasmic fractions utilizing the NP-40 protocol or lysed to prepare whole-cell extracts (Total). DNA was isolated and analyzed by qPCR for the synthesis of strong-stop HIV-1 cDNA, as described in the legend to Fig. 3. (A) M4 treatment of HeLa.LPCX control cells; (B) M4 treatment of HeLa.LPCX-HA-CPSF6-358 cells; (C) D4 treatment of HeLa.LPCX-HA-CPSF6-358 cells. Error bars denote the standard deviations from the means. The data represent those from three independent time course experiments processed in triplicate.

(30). After fractionation, greater than 95% of the mitochondrial DNA remained in the cytoplasmic fraction and greater than 90% of the 45S rRNA remained in the nuclear fraction (data not shown). The Western blot of the fractions is shown in Fig. 8G; the double-detergent fractionation procedure was compared with the NP-40 fractionation procedure used earlier, where the nuclear fraction would also contain perinuclear material. In the NP-40 and double-detergent fractionation procedures, beta-tubulin (cytoplasmic marker), lamin A/C (nuclear marker), and Nup98 (inner nuclear membrane marker) were found exclusively in the expected compartments. In contrast, the outer nuclear membrane marker Nup214 (on the cytoplasmic side of the nuclear pore) was associated exclusively with the nuclear fraction following the NP-40 protocol, but over half of the Nup214 was associated with the C+P fraction following the double-detergent protocol. These results confirmed removal of perinuclear material from the nuclei by the double-detergent wash.

We infected HeLa.LPCX cells with VSV-G-pseudotyped HIV-1 vector HR-E and compared three fractionation procedures: (i) the NP-40 protocol used for the assays whose results are presented in Fig. 3 to 7 (fractionation protocol 1), (ii) lysis of cells by swelling in hypotonic buffer followed by Dounce homogenization (fractionation protocol 2), and (ii) treatment of nuclei obtained from fractionation protocol 2 with double detergent, where the resulting postnuclear supernatant was combined with the cytoplasmic fraction (fractionation protocol 3). Fractionation protocol 2 gave cytoplasmic and nuclear plus perinuclear (N+P) fractions, while fractionation protocol 3 gave cytoplasmic plus perinuclear (C+P) and nuclear fractions. The presence of viral cDNA in all of the fractions at different time points was assessed by qPCR, as described above (Fig. 8). The patterns of strong-stop cDNA accumulation were similar for fractionation protocols 1 and 2, with rapid early accumulation in the cytoplasm followed by transfer to the nuclei beginning at 4 h (Fig. 8A, cytoplasmic and nuclear fractions; Fig. 8B, cytoplasmic versus N+P fractions). In contrast, fractionation protocol 3 gave somewhat different results, with more prolonged detection in the C+P fraction and slower accumulation in the nuclear fraction (Fig. 8B). Similar results were obtained for the intermediate and late products (Fig. 8C to F). For the first two protocols, both intermediate and full-length products of reverse transcription were found largely in the nuclear fraction. However, in the third protocol, where nuclei were washed with double detergent, intermediate and full-length cDNAs were also detected in the C+P fraction, and their levels actually increased up to 12 h postinfection. Thereafter, the cytoplasmic intermediate and full-length cDNAs declined by 24 h postinfection, suggesting the completion of nuclear entry. The double-detergent step in fractionation protocol 3 removed peri-

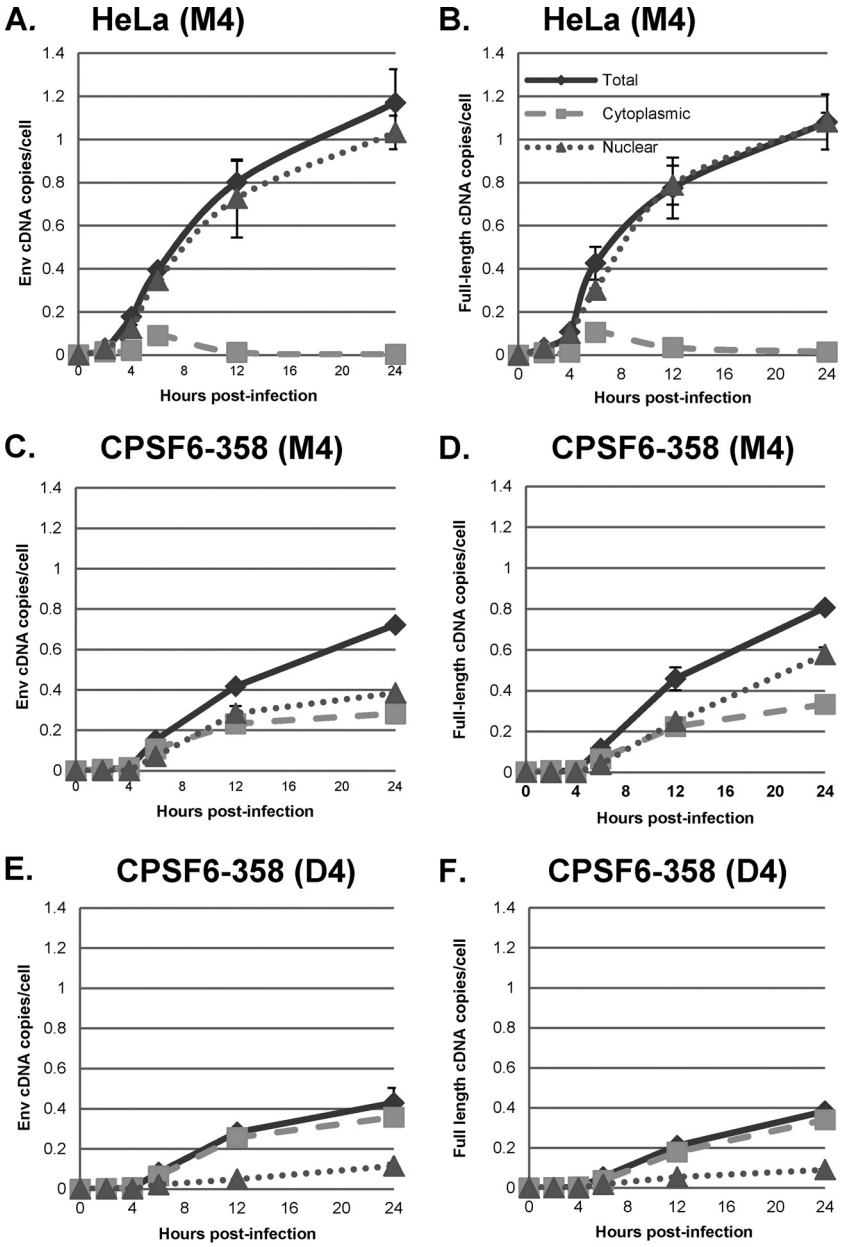

FIG 7 Effects of nuclear entry and DBR1 inhibition on HIV-1 envelope and full-length cDNA synthesis. DNAs from the same cell fractions used for the assays whose results are presented in Fig. 6 were analyzed by qPCR for the synthesis of *env* and full-length cDNA products, as described in the legend to Fig. 3. (A, C, and E) *env* reverse transcripts in M4-treated HeLa.LPCX control cells (A), M4-treated HeLa.LPCX-HA-CPSF6-358 cells (C), and D4-treated HeLa.LPCX-HA-CPSF6-358 cells (E); (B, D, and F) full-length cDNAs in M4-treated control cells (B), M4-treated HeLa.LPCX-HA-CPSF6-358 cells (D), and D4-treated HeLa.LPCX-HA-CPSF6-358 cells (F). Error bars denote the standard deviations from the means. The data represent those from three independent time course experiments processed in triplicate.

nuclear cytoplasm from the nuclei (as well as any unbroken cells), so the difference between fractionation protocols 2 and 3 suggested that the synthesis of intermediate and late viral cDNAs can take place either in the perinuclear region prior to nuclear entry or in the nucleus.

Effects of blocking of HIV-1 trafficking to the nucleus and inhibition of DBR1 on nuclear and perinuclear cDNA synthesis. To more precisely assess the effects of DBR1 inhibition and blocking of nuclear entry on HIV-1 cDNA synthesis, we transfected control HeLa cells or HeLa cells expressing CPSF6-358 with D4 or M4 for 48 h and then infected the cells with the VSV-G-pseudotyped plasmid pHR-E and harvested the cells at 2 to 24 h postinfection. Cells were fractionated with the double-detergent protocol to give nuclear and C+P fractions, as described above, and HIV-1 cDNA was assessed by qPCR (Fig. 9 and 10) The patterns of strong-stop cDNA accumulation with the double-detergent fractionation procedure were largely the same as those shown in Fig. 3, 6, and 8 (Fig. 9A and B and 10A and B). Unlike what was observed with NP-40-derived fractions, however, in the double-detergent protocol-derived C+P fractions, the synthesis of intermediate

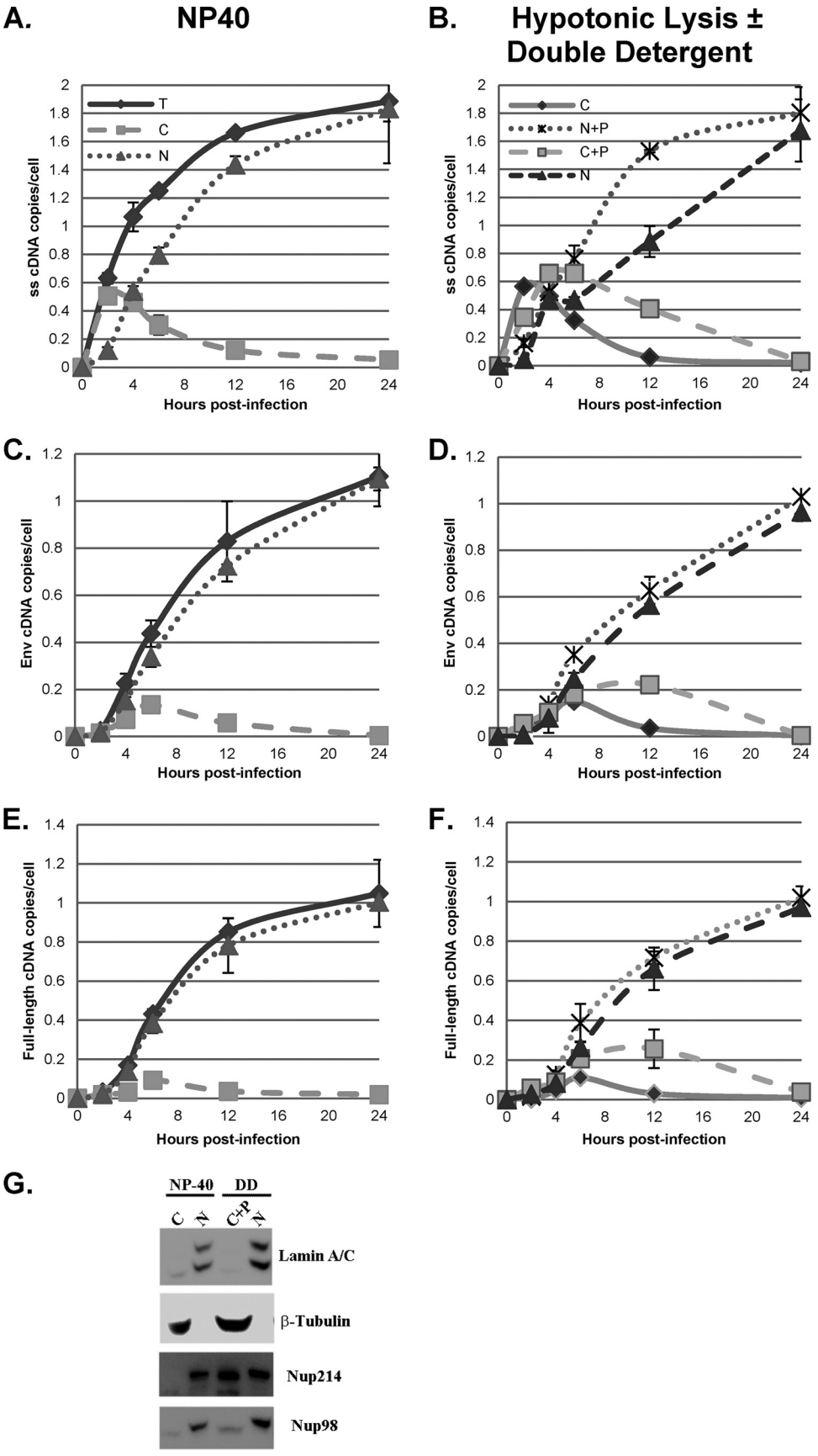
A.
NP40
T
C
N
ss cDNA copies/cell
Hours post-infection
B.
Hypotonic Lysis ±
Double Detergent
C
N+P
C+P
N
ss cDNA copies/cell
Hours post-infection
C.
Env cDNA copies/cell
Hours post-infection
D.
Env cDNA copies/cell
Hours post-infection
E.
Full-length cDNA copies/cell
Hours post-infection
F.
Full-length cDNA copies/cell
Hours post-infection
G.
NP-40
DD
C
N
C+P
N
Lamin A/C
β-Tubulin
Nup214
Nup98

and late cDNAs in the control cells (M4) was reduced by about 50% by DBR1 knockdown (D4). Since these products are largely obtained from perinuclear material, the results suggested that DBR1 can participate in the completion of cDNA synthesis in RTCs in the perinuclear region.

When infected HeLa cells expressing CPSF6-358 (and transfected with the control M4 plasmid) were analyzed by the double-detergent fractionation procedure, the intermediate and late reverse transcription products that accumulated in the C+P fraction represented higher proportions of the total cDNA (compare Fig. 7C and D with Fig. 9D and E). This indicated that some of the RTCs in CPSF6-358-expressing cells were likely accumulating at the perinuclear region and completing reverse transcription there. When CPSF6-358-expressing cells were also treated with the D4 DBR1 shRNA, there was a ca. 50% reduction in the accumulation of intermediate and full-length cDNA in the nucleus, while accumulation in the cytoplasm (C+P) was less affected (compare Fig. 9D and F with Fig. 10D and F). This might suggest that, unlike the situation in control HeLa cells, some of the perinuclear RTCs accumulating in CPSF6-358-expressing cells are completing reverse transcription without the involvement of DBR1.

DISCUSSION

In this study, we confirmed the findings of our earlier work showing that DBR1 shRNA-mediated inhibition of HIV-1 replication occurs after minus-strand strong-stop cDNA synthesis but prior to reverse transcription of the *env* gene or the completion of cDNA synthesis (14). We extended the previous studies significantly by using qPCR and cellular fractionation to study the intracellular location of different steps in reverse transcription and the role of DBR1. We found that while minus-strand strong-stop cDNA formation initially takes place in the cytoplasm, minus-strand transfer and the completion of reverse transcription take place in the nucleus or in the perinuclear region under the conditions used at an MOI near 1. Furthermore, when we inhibited viral nuclear import by CPSF6-358 expression in dividing HeLa cells, the completion of late steps in reverse transcription in the cytoplasm or perinuclear regions was enhanced. Moreover, nuclear completion of full-length cDNA synthesis was dependent on DBR1, while cytoplasmic completion of cDNA synthesis in CPSF6-358-expressing cells was not; perinuclear completion of cDNA synthesis appeared to be sensitive to DBR1 knockdown in control HeLa cells but less so in CPSF6-358-expressing cells. Our results suggest that there are two mechanisms for the completion of HIV-1 cDNA synthesis. In the predominant mechanism under our experimental conditions, the completion of reverse transcription occurs in the nucleus or in the perinuclear region and requires DBR1, perhaps to resolve an RNA structure such as a lariat to allow the completion of reverse transcription. In the second mechanism, which is enhanced in CPSF6-358-expressing cells, the completion of reverse transcription occurs in the cytoplasm and is DBR1 independent; whether the configuration of the template RNA genome is the same for these two mechanisms remains to be determined.

During reverse transcription there is typically a kinetic delay in first-strand transfer (which may be enhanced by low concentrations of deoxynucleoside triphosphates [dNTPs]), after which synthesis of posttransfer minus-strand DNA continues at a rate of 150 to 189 bases/min (31). Moreover, it has been reported that cellular factors improve endogenous reverse transcription *in vitro* by facilitating DNA strand transfer (32, 33). It will be interesting to test if DBR1 can facilitate strand transfer in such reactions. Recent studies have also demonstrated that mutations in the U3 region of the viral genome affect the synthesis of late reverse transcription products but not minus-strand strong-stop DNA (34–36). Piekna-Przybylska et al. suggested that a tRNA-like sequence in the U3 region may facilitate strand transfer by interacting with the tRNA primer to bring the 3′ and 5′ ends of viral RNA together (35). Similarly, Beerens and Kjems suggested that a circular conformation of the viral RNA genome may stimulate strand transfer by bringing the 5′ and 3′ R-region sequences in close proximity to one another (34). These data are consistent with a mechanism that brings these two regions of the genomic RNA together independently of base pairing of the 5′ and 3′ R regions in a structure that might resemble an RNA lariat; DBR1 might then facilitate the completion of reverse transcription by resolving this structure.

Despite the prevailing view that retroviral reverse transcription and the generation of the preintegration complex (PIC) take place in the cytoplasm, followed by transport to the nucleus, our results are consistent with those of prior studies of nuclear transport and accumulation of unintegrated HIV-1 DNA (28, 37–41). In activated T cells, HIV-1 minus-strand strong-stop DNA formation has been shown to take less than 6 h, while the completion of cDNA synthesis takes up to 16 h; both processes are more rapid in a T lymphoblastoid cell line (16, 31). On the other hand, by 2 h postinfection, most HIV-1 particles have reached the nucleus via microtubule- and actin filament-directed mechanisms (37, 38, 41). Other studies have demonstrated that HIV-1 matrix protein and cDNA can be found in the nucleus by 4 h postinfection (28, 40). Kim et al. detected full-length linear HIV-1 DNA in both the cytoplasmic and nuclear fractions at 5 h postinfection, while circular viral DNA was detected exclusively in the nuclear fraction at 8 to 12 h postinfection (42). Moreover, the majority of the HIV-1 DNA was detected in the nuclear fractions at all time points. Likewise, Barbosa et al. reported that cytoplasmic full-length HIV-1

FIG 8 Comparison of fractionation protocols. HeLa cells were infected with a DNase-treated HIV-1 vector (HR-E). Zero to 24 h later, the cells were lysed to prepare whole-cell (total [T]) fractions or fractionated into nuclei (N) and cytoplasm (C) utilizing the NP-40 protocol (NP-40) (A, C, and E). DNA was isolated for qPCR and analyzed with primers specific for strong-stop (A), *env* (C), and full-length (E) DNA (Fig. 3). The strong-stop, *env*, and full-length DNA copy numbers were normalized to the number of copies of either the β-globin DNA (for total and nuclear fractions) or mitochondrial DNA (for the cytoplasmic fraction) standards. Error bars denote the standard deviations from the means. The data represent those from two independent time course experiments processed in triplicate. Similarly infected cells were fractionated by hypotonic swelling and Dounce homogenization and separated into cytoplasmic (C) and nuclear plus perinuclear (N+P) fractions (B, D, and F). In parallel samples, the N+P fractions were treated with double detergent, and the supernatants were combined with the cytoplasmic fractions to give cytoplasmic plus perinuclear (C+P) and nuclear (N) fractions (results are also shown in panels B, D, and F). qPCR for strong-stop, *env*, and full-length DNA was performed. (G) Proteins from the nuclear and cytoplasmic fractions obtained by NP-40 lysis and from the N and C+P fractions obtained by fractionation with hypotonic lysis and double-detergent (DD) washing of nuclei were analyzed by SDS-PAGE and Western blotting for lamin A/C, β-tubulin, Nup214, and Nup98. Fractions from equal numbers of cells were analyzed.

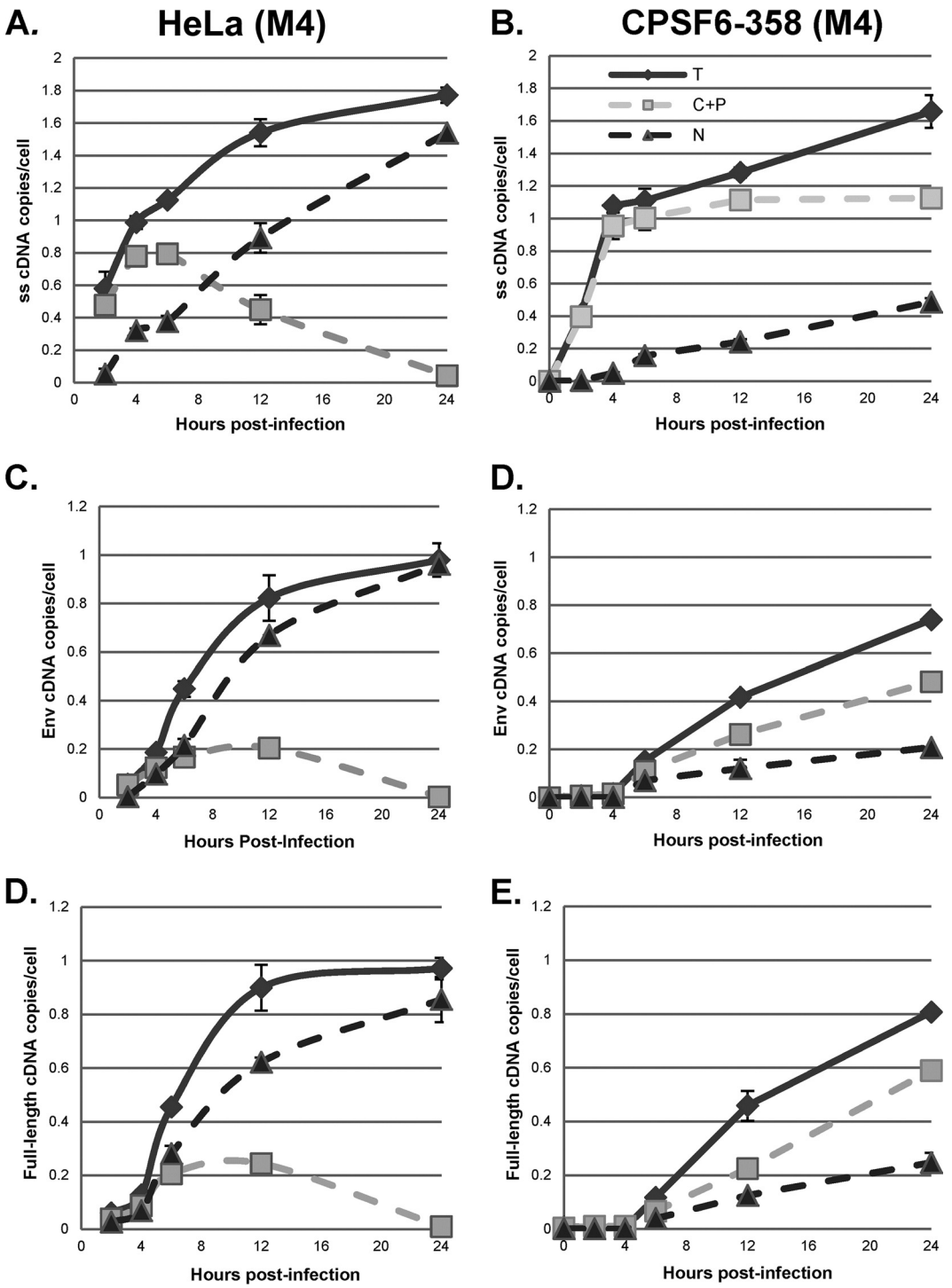

FIG 9 CPSF6-358 inhibition of nuclear entry and subcellular localization of reverse transcription products. HeLa.LPCX (HeLa) and HeLa.LPCX-HA-CPSF6-358 (CPSF6-358) cells were transfected with M4 for 48 h, followed by infection with a DNase-treated HIV-1 vector (HR-E). Zero to 24 h later, the cells were either fractionated by the double-detergent method to give nuclear (N) and C+P fractions or lysed to prepare whole-cell (total [T]) fractions. DNA was extracted and analyzed by qPCR for synthesis of strong-stop, *env*, and full-length cDNAs as described in the legend to Fig. 3. Error bars denote the standard deviations from the means. The data represent those from two independent time course experiments processed in triplicate.

DNA accounted for 30% of total DNA at 4 h but that its proportion rapidly fell to 15%, 7%, and 3% of total DNA at 8, 12, and 24 h, respectively (39). The findings of these previous studies and the results reported here are all consistent with reverse transcription initiating in the cytoplasm and continuing up to minus-strand strong-stop DNA formation in that compartment. The completion of full-length cDNA synthesis can then either occur in the perinuclear region with rapid transport into the nucleus or be

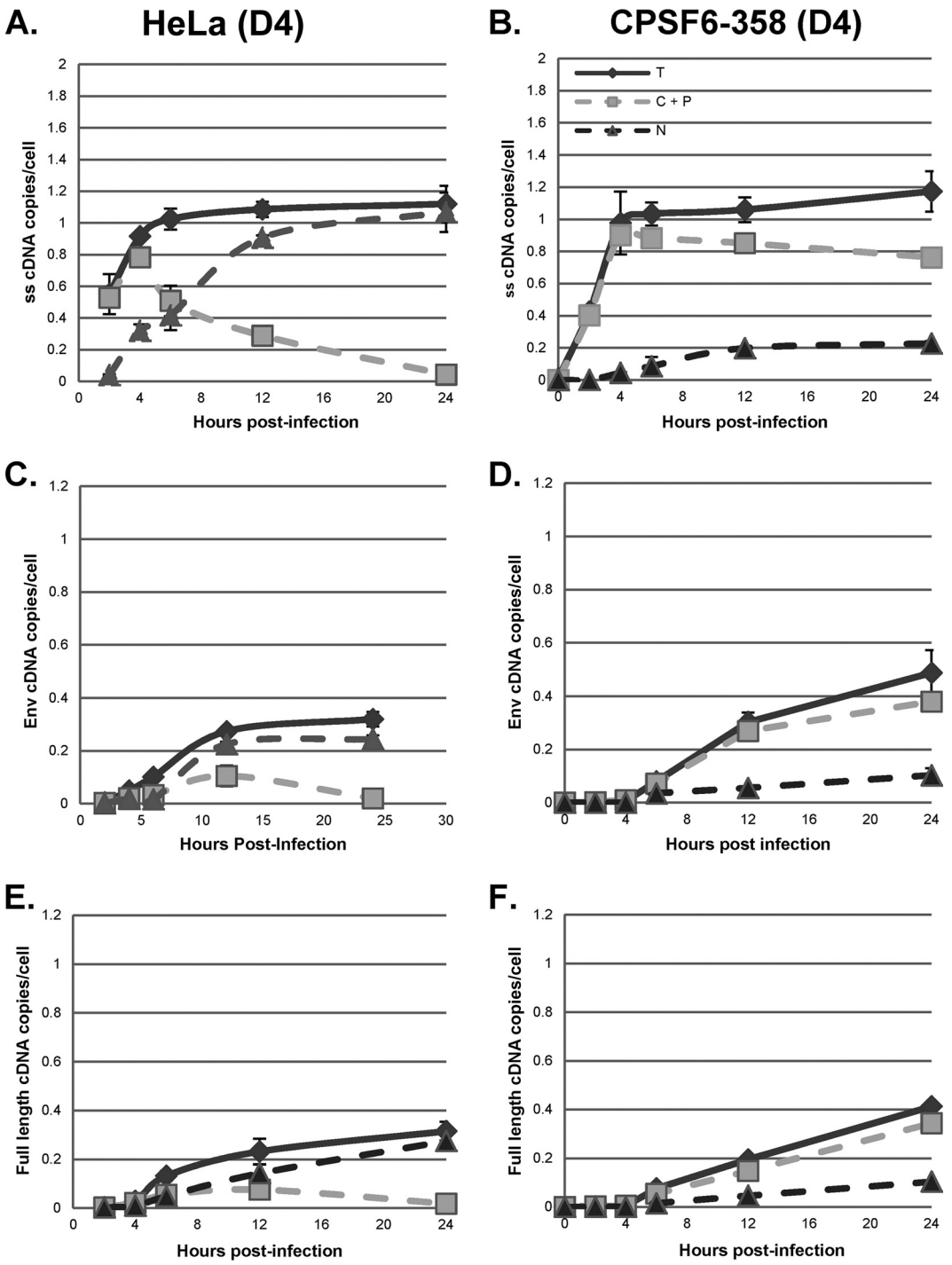

FIG 10 CPSF6-358 inhibition of nuclear entry, DBR1 shRNA inhibition, and subcellular localization of reverse transcription products. HeLa.LPCX (HeLa) and HeLa.LPCX-HA-CPSF6-358 (CPSF6-358) cells were transfected with D4 for 48 h, followed by infection with a DNase-treated HIV-1 vector (HR-E). The analysis was the same as that described in the legend to Fig. 9.

completed in the nucleus itself. Our studies are the first to distinguish nuclear and perinuclear cDNA through the use of double-detergent treatment of nuclear fractions.

While the studies reported here indicate that under these conditions, steps in HIV-1 reverse transcription after minus-strand transfer take place in the nucleus or perinuclear region, in other situations, the completion of reverse transcription can clearly occur independently of the nucleus. Indeed, full-length reverse transcripts can be obtained inefficiently from *in vitro* endogenous reverse transcription reactions of cell-free virions when dNTP concentrations are high (43). In addition, studies of mouse leukemia virus (MLV), avian leukosis virus (ALV), and HIV integration

in vitro have employed PICs obtained from the cytoplasmic fractions of infected cells. In these studies, however, infections were often performed at a much higher MOI to generate sufficient quantities of PICs for analysis and nuclear or perinuclear contents were not rigorously excluded from the cytoplasmic fractions (44–47). Mechanisms for the transport of RTCs to the perinuclear region and nucleus may have been saturated by the large amounts of virus in the infected cells. Moreover, cytoplasmic ALV DNA is less competent at *in vitro* integration than nuclear DNA when isolated in the presence of dideoxynucleotides, but otherwise, reverse transcription is completed during isolation and/or during the *in vitro* integration assay (45). In all these studies, therefore, the significant levels of integration-competent retroviral DNA detected in the cytoplasm might have been related to the high MOI, the impurity of the cytoplasmic fraction, or the completion of reverse transcription *in vitro*. Likewise, in resting $CD4^+$ T cells infected at a low MOI, the lack of ATP and/or nuclear trafficking limits RTC access to the nucleus, and therefore, full-length cDNA accumulates in the cytoplasm (48, 49). As was also shown in this report, when the nuclear import of RTCs was inhibited in HeLa cells expressing CPSF6-358, this resulted in substantially increased levels of completion of intermediate and late cDNA synthesis in the cytoplasm as well as the perinuclear regions. Moreover, the completion of cDNA synthesis in the cytoplasm was largely independent of DBR1, since it was not affected by shRNA knockdown of DBR1. Thus, the completion of HIV reverse transcription can take place in different cellular compartments, depending on the conditions of infection and the physiology of the infected cells.

Studies on the nuclear import of HIV RTCs have demonstrated that the completion of reverse transcription is not a requirement for nuclear entry (50, 51). Zaitseva et al. reported that viral RNA accumulated within the nuclei of cells infected with a reverse transcription-deficient HIV-1 mutant (50). Interestingly, when we followed the viral RNA genome in infected cells, viral RNA, measured by quantitative reverse transcription-PCR for the 3′ region, accumulated in the nucleus under conditions of DBR1 knockdown. This is consistent with the transport of RTCs to the nucleus, despite the block to the completion of reverse transcription and template degradation by the RNase H activity of RT in the absence of DBR1. Bukrinsky and colleagues also previously showed that RTCs can complete reverse transcription in both the cytoplasm and the nucleus (51). The latter study also concluded that RTCs that completed reverse transcription in the nucleus were defective for integration (51). Our study did not examine the integration competency of the viral DNA that was produced in the nucleus versus that of the viral DNA that was produced in the cytoplasm, although under our conditions, essentially all intermediate and late reverse transcription occurred in the nuclear or perinuclear fractions. Under these conditions, the VSV-G-pseudotyped H-RE vector and the clinical HIV isolate are infectious in GHOST-R5X4 and HeLa cells. Moreover, we previously reported that inhibition of DBR1 has an effect on HIV replication (14). It is possible that there is more than one pathway for the transport of RTCs to the nucleus and that these pathways may have different requirements for cellular factors such as DBR1 in generating infectious viral DNAs, as well as potentially different efficiencies of productive infection.

The possibility that the HIV-1 genomic RNA adopts a lariat-like form during reverse transcription is controversial. While the results presented in this study are consistent with such a process, they are not dependent on it. These experiments indicate a role for DBR1 in the completion of nuclear or perinuclear HIV-1 reverse transcription at or after the step of minus-strand transfer, regardless of whether lariat formation of genomic RNA occurs or not. Further studies to address the structure of the viral RNA during reverse transcription are in progress.

In conclusion, we confirmed that DBR1 shRNA inhibits HIV-1 reverse transcription during or after the minus-strand template switch. Moreover, we found that under the conditions used here at an MOI of 1, initiation of reverse transcription takes place in the cytoplasm, but the completion of reverse transcription largely takes place in the nucleus or perinuclear region. Blocking nuclear transport of viral RTCs with CPSF6-358 results in detectable cytoplasmic full-length cDNA. DBR1 appears to be required for the completion of nuclear and perinuclear cDNA synthesis but not for full-length cDNA formation in the cytoplasm. Characterization and identification of additional factors that are involved in minus-strand transfer should provide new insight into this early step in reverse transcription and may also provide clues to the development of new therapeutics.

ACKNOWLEDGMENTS

This work was supported in part by grant ID07-I-124 from the California HIV-AIDS Research Program to D. Camerini. The support of the UCI Cancer Research Institute and the Chao Family Comprehensive Cancer Center is acknowledged. A. E. Galvis was supported by the UCI Medical Scientist Training Program, grant T32-GM08620. T. Nitta was supported by a Japan Society for the Promotion of Science postdoctoral fellowship for research abroad.

REFERENCES

1. **Telesnitsky A, Goff SP.** 1997. Reverse transcriptase and generation of retroviral DNA. *In* Coffin JM, Hughes SH, Varmus HE (ed), Retroviruses. Cold Spring Harbor Laboratory Press, Cold Spring Harbor, NY.
2. **Dang Q, Hu WS.** 2001. Effects of homology length in the repeat region on minus-strand DNA transfer and retroviral replication. J. Virol. **75:**809–820. http://dx.doi.org/10.1128/JVI.75.2.809-820.2001.
3. **Tisdale M, Schulze T, Larder BA, Moelling K.** 1991. Mutations within the RNase H domain of human immunodeficiency virus type 1 reverse transcriptase abolish virus infectivity. J. Gen. Virol. **72**(Pt 1):59–66. http://dx.doi.org/10.1099/0022-1317-72-1-59.
4. **Le Grice SFJ.** 2003. "In the beginning": initiation of minus strand dna synthesis in retroviruses and LTR-containing retrotransposons. Biochemistry **42:**14349–14355. http://dx.doi.org/10.1021/bi030201q.
5. **Gilboa E, Mitra SW, Goff S, Baltimore D.** 1979. A detailed model of reverse transcription and tests of crucial aspects. Cell **18:**93–100. http://dx.doi.org/10.1016/0092-8674(79)90357-X.
6. **Karst SM, Rütz ML, Menees TM.** 2000. The yeast retrotransposons Ty1 and Ty3 require the RNA lariat debranching enzyme, Dbr1p, for efficient accumulation of reverse transcripts. Biochem. Biophys. Res. Commun. **268:**112–117. http://dx.doi.org/10.1006/bbrc.1999.2048.
7. **Chapman KB, Boeke JD.** 1991. Isolation and characterization of the gene encoding yeast debranching enzyme. Cell **65:**483–492. http://dx.doi.org/10.1016/0092-8674(91)90466-C.
8. **Cheng Z, Menees TM.** 2004. RNA branching and debranching in the yeast retrovirus-like element Ty1. Science **303:**240–243. http://dx.doi.org/10.1126/science.1087023.
9. **Roth JF.** 2000. The yeast Ty virus-like particles. Yeast **16:**785–795.
10. **Coombes CE, Boeke JEFD.** 2005. An evaluation of detection methods for large lariat RNAs. RNA **11:**323–331. http://dx.doi.org/10.1261/rna.7124405.
11. **Salem LA, Boucher CL, Menees TM.** 2003. Relationship between RNA lariat debranching and Ty1 element retrotransposition. J. Virol. **77:**12795–12806. http://dx.doi.org/10.1128/JVI.77.23.12795-12806.2003.
12. **Marr SF, Telesnitsky A.** 2003. Mismatch extension during strong stop strand transfer and minimal homology requirements for replicative template switch-

ing during Moloney murine leukemia virus replication. J. Mol. Biol. **330:**657–674. http://dx.doi.org/10.1016/S0022-2836(03)00597-7.
13. **Klaver B, Berkhout B.** 1994. Premature strand transfer by the HIV-1 reverse transcriptase during strong-stop DNA synthesis. Nucleic Acids Res. **22:**137–144. http://dx.doi.org/10.1093/nar/22.2.137.
14. **Ye Y, De Leon J, Yokoyama N, Naidu Y, Camerini D.** 2005. DBR1 siRNA inhibition of HIV-1 replication. Retrovirology **2:**63. http://dx.doi.org/10.1186/1742-4690-2-63.
15. **Ruskin B, Krainer AR, Maniatis T, Green MR.** 1984. Excision of an intact intron as a novel lariat structure during pre-mRNA splicing in vitro. Cell **38:**317–331. http://dx.doi.org/10.1016/0092-8674(84)90553-1.
16. **Zack J, Haislip A, Krogstad P, Chen I.** 1992. Incompletely reverse-transcribed human immunodeficiency virus type 1 genomes in quiescent cells can function as intermediates in the retroviral life cycle. J. Virol. **66:**1717–1725.
17. **Berlivet S, Houlard M, Gérard M.** 2010. Loss-of-function studies in mouse embryonic stem cells using the pHYPER shRNA plasmid vector. Methods Mol. Biol. **650:**85–100. http://dx.doi.org/10.1007/978-1-60761-769-3_7.
18. **Berlivet S, Guiraud V, Houlard M, Gérard M.** 2007. pHYPER, a shRNA vector for high-efficiency RNA interference in embryonic stem cells. Biotechniques **42:**738–740. http://dx.doi.org/10.2144/000112454.
19. **Zufferey R, Dull T, Mandel RJ, Bukovsky A, Quiroz D, Naldini L, Trono D.** 1998. Self-inactivating lentivirus vector for safe and efficient in vivo gene delivery. J. Virol. **72:**9873–9880.
20. **Zufferey R, Nagy D, Mandel RJ, Naldini L, Trono D.** 1997. Multiply attenuated lentiviral vector achieves efficient gene delivery in vivo. Nat. Biotechnol. **15:**871–875. http://dx.doi.org/10.1038/nbt0997-871.
21. **Choudhary SK, Choudhary NR, Kimbrell KC, Colasanti J, Ziogas A, Kwa D, Schuitemaker H, Camerini D.** 2005. R5 human immunodeficiency virus type 1 infection of fetal thymic organ culture induces cytokine and CCR5 expression. J. Virol. **79:**458–471. http://dx.doi.org/10.1128/JVI.79.1.458-471.2005.
22. **Mörner, A, Björndal Å, Albert J, KewalRamani VN, Littman DR, Inoue R, Thorstensson R, Fenyö EM, Björling, E.** 1999. Primary human immunodeficiency virus type 2 (HIV-2) isolates, like HIV-1 isolates, frequently use CCR5 but show promiscuity in coreceptor usage. J. Virol. **73:**2343–2349.
23. **Lee KE, Ambrose Z, Martin TD, Oztop I, Mulky A, Julias JG, Vandegraaff N, Baumann JG, Wang R, Yuen W, Takemura T, Shelton K, Taniuchi I, Li Y, Sodroski J, Littman DR, Coffin JM, Hughes SH, Unutmaz D, Engelman A, KewalRamani VN.** 2010. Flexible use of nuclear import pathways by HIV-1. Cell Host Microbe **7:**221–233. http://dx.doi.org/10.1016/j.chom.2010.02.007.
24. **Holtzman E, Smith I, Penman S.** 1966. Electron microscopic studies of detergent-treated HeLa cell nuclei. J. Mol. Biol. **17:**131–135. http://dx.doi.org/10.1016/S0022-2836(66)80099-2.
25. **Penman S.** 1966. RNA metabolism in the HeLa cell nucleus. J. Mol. Biol. **17:**117–130. http://dx.doi.org/10.1016/S0022-2836(66)80098-0.
26. **Sambrook J, Russell DW.** 2001. Molecular cloning: a laboratory manual, 3rd ed. Cold Spring Harbor Laboratory Press, Cold Spring Harbor, NY.
27. **Uemura M, Zheng Q, Koh C, Nelson W, Yegnasubramanian S, De Marzo A.** 2012. Overexpression of ribosomal RNA in prostate cancer is common but not linked to rDNA promoter hypomethylation. Oncogene **31:**1254–1263. http://dx.doi.org/10.1038/onc.2011.319.
28. **Zennou V, Petit C, Guetard D, Nerhbass U, Montagnier L, Charneau P.** 2000. HIV-1 genome nuclear import is mediated by a central DNA flap. Cell **101:**173–185. http://dx.doi.org/10.1016/S0092-8674(00)80828-4.
29. **Fontoura BMA, Blobel G, Matunis MJ.** 1999. A conserved biogenesis pathway for nucleoporins: proteolytic processing of a 186-kilodalton precursor generates Nup98 and the novel nucleoporin, Nup96. J. Cell Biol. **144:**1097–1112. http://dx.doi.org/10.1083/jcb.144.6.1097.
30. **Kraemer D, Wozniak RW, Blobel G, Radu A.** 1994. The human CAN protein, a putative oncogene product associated with myeloid leukemogenesis, is a nuclear pore complex protein that faces the cytoplasm. Proc. Natl. Acad. Sci. U. S. A. **91:**1519–1523. http://dx.doi.org/10.1073/pnas.91.4.1519.
31. **Karageorgos L, Li P, Burrell CJ.** 1995. Stepwise analysis of reverse transcription in a cell-to-cell human immunodeficiency virus infection model: kinetics and implications. J. Gen. Virol. **76:**1675–1686. http://dx.doi.org/10.1099/0022-1317-76-7-1675.
32. **Warrilow D, Meredith L, Davis A, Burrell C, Li P, Harrich D.** 2008. Cell factors stimulate human immunodeficiency virus type 1 reverse transcription in vitro. J. Virol. **82:**1425–1437. http://dx.doi.org/10.1128/JVI.01808-07.
33. **Warrilow D, Warren K, Harrich D.** 2010. Strand transfer and elongation of HIV-1 reverse transcription is facilitated by cell factors in vitro. PLoS One **5:**e13229. http://dx.doi.org/10.1371/journal.pone.0013229.
34. **Beerens N, Kjems J.** 2010. Circularization of the HIV-1 genome facilitates strand transfer during reverse transcription. RNA **16:**1226–1235. http://dx.doi.org/10.1261/rna.2039610.
35. **Piekna-Przybylska D, Dykes C, Demeter LM, Bambara RA.** 2011. Sequences in the U3 region of human immunodeficiency virus 1 improve efficiency of minus strand transfer in infected cells. Virology **410:**368–374. http://dx.doi.org/10.1016/j.virol.2010.11.026.
36. **Piekna-Przybylska D, Bambara RA.** 2011. Requirements for efficient minus strand strong-stop DNA transfer in human immunodeficiency virus 1. RNA Biol. **8:**230–236. http://dx.doi.org/10.4161/rna.8.2.14802.
37. **Arhel NJ, Souquere-Besse S, Munier S, Souque P, Guadagnini S, Rutherford S, Prévost MC, Allen TD, Charneau P.** 2007. HIV-1 DNA Flap formation promotes uncoating of the pre-integration complex at the nuclear pore. EMBO J. **26:**3025–3037. http://dx.doi.org/10.1038/sj.emboj.7601740.
38. **Arhel N, Genovesio A, Kim KA, Miko S, Perret E, Olivo-Marin JC, Shorte S, Charneau P.** 2006. Quantitative four-dimensional tracking of cytoplasmic and nuclear HIV-1 complexes. Nat. Methods **3:**817–824. http://dx.doi.org/10.1038/nmeth928.
39. **Barbosa P, Charneau P, Dumey N, Clavel F.** 1994. Kinetic analysis of HIV-1 early replicative steps in a coculture system. AIDS Res. Hum. Retroviruses **10:**53–59. http://dx.doi.org/10.1089/aid.1994.10.53.
40. **Bukrinskaya A, Brichacek B, Mann A, Stevenson M.** 1998. Establishment of a functional human immunodeficiency virus type 1 (HIV-1) reverse transcription complex involves the cytoskeleton. J. Exp. Med. **188:**2113–2125. http://dx.doi.org/10.1084/jem.188.11.2113.
41. **McDonald D, Vodicka MA, Lucero G, Svitkina TM, Borisy GG, Emerman M, Hope TJ.** 2002. Visualization of the intracellular behavior of HIV in living cells. J. Cell Biol. **159:**441–452. http://dx.doi.org/10.1083/jcb.200203150.
42. **Kim S, Byrn R, Groopman J, Baltimore D.** 1989. Temporal aspects of DNA and RNA synthesis during human immunodeficiency virus infection: evidence for differential gene expression. J. Virol. **63:**3708–3713.
43. **Zhang H, Dornadula G, Pomerantz RJ.** 1996. Endogenous reverse transcription of human immunodeficiency virus type 1 in physiological microenvironments: an important stage for viral infection of nondividing cells. J. Virol. **70:**2809–2824.
44. **Engelman A, Oztop I, Vandegraaff N, Raghavendra NK.** 2009. Quantitative analysis of HIV-1 preintegration complexes. Methods **47:**283–290. http://dx.doi.org/10.1016/j.ymeth.2009.02.005.
45. **Lee Y, Coffin JM.** 1991. Relationship of avian retrovirus DNA synthesis to integration in vitro. Mol. Cell. Biol. **11:**1419–1430.
46. **Farnet CM, Haseltine WA.** 1990. Integration of human immunodeficiency virus type 1 DNA in vitro. Proc. Natl. Acad. Sci. U. S. A. **87:**4164–4168. http://dx.doi.org/10.1073/pnas.87.11.4164.
47. **Brown PO, Bowerman B, Varmus HE, Bishop JM.** 1987. Correct integration of retroviral DNA in vitro. Cell **49:**347–356. http://dx.doi.org/10.1016/0092-8674(87)90287-X.
48. **Stevenson M, Stanwick T, Dempsey M, Lamonica C.** 1990. HIV-1 replication is controlled at the level of T cell activation and proviral integration. EMBO J. **9:**1551–1560.
49. **Bukrinsky MI, Sharova N, Dempsey MP, Stanwick TL, Bukrinskaya AG, Haggerty S, Stevenson M.** 1992. Active nuclear import of human immunodeficiency virus type 1 preintegration complexes. Proc. Natl. Acad. Sci. U. S. A. **89:**6580–6584. http://dx.doi.org/10.1073/pnas.89.14.6580.
50. **Zaitseva L, Cherepanov P, Leyens L, Wilson SJ, Rasaiyaah J, Fassati A.** 2009. HIV-1 exploits importin 7 to maximize nuclear import of its DNA genome. Retrovirology **6:**11. http://dx.doi.org/10.1186/1742-4690-6-11.
51. **Iordanskiy S, Berro R, Altieri M, Kashanchi F, Bukrinsky M.** 2006. Intracytoplasmic maturation of the human immunodeficiency virus type 1 reverse transcription complexes determines their capacity to integrate into chromatin. Retrovirology **3:**4. http://dx.doi.org/10.1186/1742-4690-3-4.